Filterbank-Based Blind Code Synchronization for DS-CDMA Systems in Multipath Fading Channels

Hongbin Li, *Member, IEEE*, and Rensheng Wang

***Abstract*—We present a filterbank approach to blind code synchronization for asynchronous direct-sequence (DS) code-division multiple-access (CDMA) systems. The key idea of the proposed scheme is to first pass the received signal through a bank of filters, which are designed to enhance signals of interest and suppress interference/noise, and then to derive the code timing from the filtered data. The only required knowledge by the proposed filterbank scheme is the spreading code of the desired user. It can be used in various environments, including frequency-nonselective and frequency-selective, time-invariant, and time-varying fading channels. It can deal with colored channel noise and unmodeled interference, such as inter-cell interference (ICI) and narrowband interference. It has relatively low complexity and can be readily implemented using standard adaptive algorithms. We show that under mild conditions, the proposed scheme yields statistically consistent [in signal-to-noise ratio (SNR)] code timing estimates, irrespective of the strength of the interference and with only a finite number of data samples. We also derive an unconditional Cramér–Rao bound (UCRB), which serves as a lower bound for all unbiased blind code synchronization schemes. Numerical results indicate that the proposed scheme compares favorably with a popular subspace-based method in terms of user capacity, near–far resistance, and robustness to time-varying fading and unmodeled interference.**

***Index Terms*—Code division multiple access, code synchronization, Cramér-Rao bound (CRB), interference suppression, parameter estimation.**

I. Introduction

Code division multiple access (CDMA) is a major air interface candidate for future wireless mobile networks [1]. In CDMA systems, all transmissions occupy the same time and frequency band. Thus, interference suppression is of paramount importance to the design of CDMA receivers. A variety of multiuser receivers resistant to multiple access interference (MAI) have been proposed (e.g., [2] and references therein). Their performance, however, relies on the availability of accurate estimates of some of the channel parameters, such as the gain, phase, and, particularly, *code timing* associated with the desired transmission.

Code synchronization, which parallels the research on multiuser detection for CDMA systems, has been receiving increasing interest recently. A variety of code synchronization techniques have been proposed so far, starting from the classical correlator-based schemes, which are optimum in a single-user environment but highly sensitive to MAI, to the more recently proposed schemes that show improved resistance to MAI and can support a larger number of active transmissions within a cell. These schemes rely on either *explicit training* or some *inherent structure* of the transmitted signal. In the latter case, the need for training may be eliminated, resulting in the so-called *blind* methods.

One interesting training-assisted code synchronization scheme is the minimum mean-squared error (MMSE) timing estimator [3]–[5]. The MMSE scheme was observed to outperform substantially the correlator-based methods, particularly in a near–far environment. The MMSE scheme requires little side information of the transmission, and its computational requirement is moderate. However, the number of active transmissions that can be supported by the MMSE scheme is relatively small [6]. Another training-assisted scheme is the large sample maximum likelihood (LSML) algorithm [7] (also see [8]). It models the MAI and channel noise as a colored Gaussian random process with an unknown covariance matrix. An estimate of the covariance matrix is used to prewhiten the received signal. The LSML algorithm achieves a larger capacity and better accuracy than the MMSE algorithm [7]. When used for multiuser synchronization, it has to estimate the covariance matrix and perform prewhitening for each user separately. Thus, the associated computational complexity is relatively high. A decoupled multiuser acquisition (DEMA) algorithm was recently proposed in [6]. It estimates the delays for all users simultaneously, resulting in not only a significantly reduced computational complexity but also in an improved capacity and accuracy than LSML [6].

Although the above training-assisted schemes perform quite well in stationary or slow-fading channels, their performance degrades considerably as the channel fading rate increases [6]. Moreover, in order to track channel variations, training symbols have to be retransmitted periodically, leading to throughput reductions. Blind schemes, on the other hand, do not suffer from such drawbacks. A well-known blind code synchronization scheme is the subspace-based method proposed in [9] and independently in [10]. The subspace method resembles the multiple signal classification (MUSIC) algorithm originally considered for direction-of-arrival (DOA) estimation in array processing [11]. It relies on the ability to decompose the observation space into orthogonal complements, which are referred to as the signal and noise subspaces. When *unknown/unmodeled* interference (e.g., inter-cell interference (ICI) and narrow-

Manuscript received November 27, 2001; revised August 27, 2002. This work was supported by the New Jersey Commission on Science and Technology and the Center for Wireless Network Security at Stevens Institute of Technology. The associate editor coordinating the review of this paper and approving it for publication was Dr. Rick S. Blum.

The authors are with the Department of Electrical and Computer Engineering, Stevens Institute of Technology, Hoboken, NJ 07030 USA (e-mail: hli@stevens-tech.edu).

Digital Object Identifier 10.1109/TSP.2002.806565

band interference in cellular overlay systems [12]) is present, or if the channel noise is *colored* with unknown correlation, subspace decomposition becomes questionable, as is the subspace-based code timing estimate (see Section V). In order to correctly separate the signal subspace from the noise subspace, the subspace method also needs to know the number of transmissions, which may be estimated by some model detection methods (e.g., [13]). It is, however, not unusual for model detection methods to underestimate or overestimate the number of transmissions by a small quantity [14]. Such a model mismatch, as we will see in Section V, may degrade the performance of the subspace method substantially. The subspace synchronization scheme was extended to the multipath fading case in [15]. A modified subspace algorithm was proposed in [16] to extend the observation interval to span several symbol durations, and an enhanced estimation accuracy was reported.

In this paper, we propose an alternative blind code synchronization scheme. The idea here is as follows: The received CDMA signal is known to be "noisy" due to the presence of MAI and possibly other sources of interference; hence, instead of directly using the raw data for timing estimation, we first pass the data through a bank of filters (or filterbank), which are designed to enhance the useful signals and suppress the interference/noise, and then derive the code timing from the filtered data. The resulting blind code synchronization scheme, or *filterbank scheme*, requires only the knowledge of the spreading code of the desired user, making it ideal for a decentralized implementation. The filterbank scheme can be used in frequency-flat and frequency-selective, time-invariant, and time-varying fading channels; it can cope effectively with colored channel noise and unknown/unmodeled interference. The filterbank scheme has a relatively low complexity and can be readily implemented using standard adaptive algorithms. Hence, it is appealing not only for code acquisition but for code tracking as well. We remark that the filterbank-based code-synchronization scheme proposed here is related to several recent studies on filterbank applications to adaptive filters [17].

The rest of the paper is organized as follows. In Section II, we introduce the general data model for CDMA systems in time-varying multipath fading channels and formulate the problem of interest. The filterbank-based blind code synchronization scheme is presented in Section III. Several attributes of the proposed scheme, including its statistical consistent property, and an unconditional Cramér-Rao bound (UCRB) for the estimation problem are discussed in Section IV; we also discuss there the relation of the proposed scheme with several existing ones, e.g., [18] and [19]. Section V contains the numerical studies. Finally, we draw conclusions in Section VI.

A. Notation

Vectors (matrices) are denoted by boldface lower (upper) case letters; all vectors are column vectors; superscripts $(\cdot)^T$, $(\cdot)^*$, and $(\cdot)^H$ denote the transpose, conjugate, and conjugate transpose, respectively; $\mathbf{I}_M$ is the $M \times M$ identity matrix; $\mathbf{0}$ is a vector or matrix with all zero elements; $E\{\cdot\}$ denotes the statistical expectation; $\|\cdot\|$ denotes the vector 2-norm [20]; tr$\{\cdot\}$ takes the trace of a matrix argument; $\otimes$ denotes the matrix Kronecker product [21]; diag$\{\cdot\}$ is a diagonal or block diagonal matrix; $\mathcal{CN}(\mathbf{m}, \mathbf{R})$ denotes a circularly symmetric complex Gaussian random vector with mean $\mathbf{m}$ and covariance matrix $\mathbf{R}$; finally, $[\mathbf{a}]_i$ (respectively, $[\mathbf{A}]_{i,j}$) denotes the ith (resp. ijth) element of vector $\mathbf{a}$ (resp., matrix $\mathbf{A}$).

II. Data Model and Problem Formulation

Consider a baseband asynchronous K-user DS-CDMA system. The transmitted signal for user k is given by

$$x_k(t) = \sum_{m=0}^{M-1} d_k(m) c_k(t - mT_s)$$

where M is the number of symbols considered for code acquisition, and $d_k(m)$ and $c_k(t)$ denote the mth symbol and spreading waveform, respectively, for user k. Here, $T_s = NT_c$ denotes the symbol interval, with T_c and N being the chip interval and *spreading gain*, respectively.

The signal $x_k(t)$ passes through a baseband *frequency-selective*, *time-varying* channel whose impulse response is modeled as [22]

$$h_k(\tau, t) = \sum_{l=1}^{L_k} \alpha_{k,l}(t) \delta(\tau - \tau_{k,l}) \tag{1}$$

where $\delta(t)$ denotes the Dirac delta function, $\alpha_{k,l}(t)$ and $\tau_{k,l}$, respectively, denote the (complex-valued) time-varying fading coefficient and the propagation delay associated with path l of user k, and L_k denotes the total number of paths of user k. The received signal is then given by

$$y(t) = \sum_{k=1}^{K} \sum_{l=1}^{L_k} \alpha_{k,l}(t) x_k(t - \tau_{k,l}) + e(t) \tag{2}$$

where $e(t)$ denotes the channel noise. In the following, we assume that the fading process $\alpha_{k,l}(t)$ is wide-sense stationary and varies slowly relative to the symbol rate so that $\alpha_{k,l}(t) \approx \alpha_{k,l}(mT_s)$ for $t \in [mT_s, (m+1)T_s)$.[1]

The receiver front-end is a chip-matched filter (CMF) whose output is sampled every $T_i = T_c/Q$ s, where $Q \geq 1$ is an integer referred to as the *oversampling factor*. Similar to previous studies (e.g., [3]–[10], [15]–[19]), we assume in the sequel rectangular chip waveforms, although generalizations to other chip waveforms are conceptually straightforward. For rectangular chip waveforms, the CMF reduces to an integrate-and-dump filter (IDF) (see, e.g., [9]).

We first form vectors $\{\mathbf{y}(m)\}_{m=0}^{M-1}$ composed of samples of the IDF output within one symbol period, i.e., $\mathbf{y}(m) = \left[y(mNQ), \ \ldots, \ y(mNQ + NQ - 1)\right]^T$. Define the spreading vector $\mathbf{c}_k \triangleq \left[c_k(0), \ \ldots, \ c_k(NQ - 1)\right]^T$, $k = 1, \ldots, K$, where $c_k(n) = 1/T_i \int_{(n-1)T_i}^{nT_i} c_k(t)dt$. Due to asynchronous transmissions, two adjacent symbols in each path contribute to $\mathbf{y}(m)$. That is, the contribution to $\mathbf{y}(m)$ from

[1]The assumption is mainly for arriving at a tractable data model. In testing the proposed scheme, we relax this assumption and allow $\alpha_{k,l}(t)$ to vary continuously within a symbol interval; see Section V.

$\alpha_{k,l}(t)x_k(t-\tau_{k,l})$ [cf. (2)] has the following form [5]–[10], [18]:

$$\alpha_{k,l}(m)d_k(m-1)\mathbf{a}_k(\tau_{k,l})+\alpha_{k,l}(m)d_k(m)\bar{\mathbf{a}}_k(\tau_{k,l}) \quad (3)$$

where $\alpha_{k,l}(m)\triangleq\alpha_{k,l}(t)|_{t=mT_s}$. As we will see later, it is convenient to express $\tau_{k,l}$ as a multiple of the sampling interval T_i

$$\tau_{k,l}=(p_{k,l}+\mu_{k,l})T_i \quad (4)$$

where $0\le p_{k,l}\le NQ-1$ is an integer, and $0\le\mu_{k,l}<1$ is a fractional number. In (4), we also implicitly assumed that $\tau_{k,l}<T_s$ [cf. (14)]. The vectors $\mathbf{a}_k(\tau_{k,l})$ and $\bar{\mathbf{a}}_k(\tau_{k,l})$ in (3) consist of linear combinations of the *acyclic left and right shift* of user k's spreading code $\mathbf{c}_k$ [10], [18]:

$$\mathbf{a}_k(\tau_{k,l})=(1-\mu_{k,l})\mathbf{c}_k^l(p_{k,l})+\mu_{k,l}\mathbf{c}_k^l(p_{k,l}+1) \quad (5)$$
$$\bar{\mathbf{a}}_k(\tau_{k,l})=(1-\mu_{k,l})\mathbf{c}_k^r(p_{k,l})+\mu_{k,l}\mathbf{c}_k^r(p_{k,l}+1) \quad (6)$$

where

$$\mathbf{c}_k^l(p_{k,l})=\left[c_k(NQ-p_{k,l}),\,\ldots,\,c_k(NQ-1),\, \mathbf{0}_{1\times(NQ-p_{k,l})}\right]^T \quad (7)$$
$$\mathbf{c}_k^r(p_{k,l})=\left[\mathbf{0}_{1\times p_{k,l}},\,c_k(0),\,\ldots,\,c_k(NQ-p_{k,l}-1)\right]^T. \quad (8)$$

To simplify the notation, let

$$b_{k,l}(m)\triangleq\alpha_{k,l}(m)d_k(m-1) \quad (9)$$
$$\bar{b}_{k,l}(m)\triangleq\alpha_{k,l}(m)d_k(m). \quad (10)$$

It follows from (3) that the vector $\mathbf{y}(m)$ can be expressed as

$$\begin{aligned}\mathbf{y}(m)&=\sum_{k=1}^{K}\sum_{l=1}^{L_k}\left[b_{k,l}(m)\mathbf{a}_k(\tau_{k,l})+\bar{b}_{k,l}(m)\bar{\mathbf{a}}_k(\tau_{k,l})\right]\\&\quad+\mathbf{e}(m),\\&=\sum_{k=1}^{K}\mathbf{A}_k(\boldsymbol{\tau}_k)\mathbf{b}_k(m)+\mathbf{e}(m)\end{aligned} \quad (11)$$

where $\mathbf{e}(m)\in\mathbb{C}^{NQ\times 1}$ consists of noise samples, $\boldsymbol{\tau}_k\triangleq\left[\tau_{k,1},\,\ldots,\,\tau_{k,L_k}\right]^T$, and

$$\mathbf{A}_k(\boldsymbol{\tau}_k)=\left[\mathbf{a}_k(\tau_{k,1}),\,\bar{\mathbf{a}}_k(\tau_{k,1}),\,\ldots,\,\mathbf{a}_k(\tau_{k,L_k})\; \bar{\mathbf{a}}_k(\tau_{k,L_k})\right] \quad (12)$$
$$\mathbf{b}_k(m)=\left[b_{k,1}(m),\,\bar{b}_{k,1}(m),\,\ldots,\,b_{k,L_k}(m)\; \bar{b}_{k,L_k}(m)\right]^T. \quad (13)$$

The problem of interest to this paper is to estimate the delay parameters $\{\boldsymbol{\tau}_k\}$. To avoid ambiguity, we assume that the path delays of the same user are *distinct*; furthermore, we assume that the delay spread is within one symbol interval such that (also see [10])

$$0\le\tau_{k,1}<\cdots<\tau_{k,L_k}<T_s. \quad (14)$$

Without loss of generality, let us assume that the first user is of interest. The problem is to estimate the path delays $\{\tau_{1,l}\}_{l=1}^{L_1}$ from the receiver output $\{\mathbf{y}(m)\}_{m=0}^{M-1}$ only (i.e., without any knowledge of the transmitted symbols). In light of the decomposition of $\{\tau_{1,l}\}_{l=1}^{L_1}$ in (4), the problem is equivalently to estimate $\{p_{1,l},\mu_{1,l}\}_{l=1}^{L_1}$.

III. Filterbank-Based Blind Code Synchronization

Assuming that the first user is of interest, we rewrite (11) as

$$\mathbf{y}(m)=\mathbf{A}_1(\boldsymbol{\tau}_1)\mathbf{b}_1(m)+\mathbf{v}(m) \quad (15)$$

where $\mathbf{v}(m)$ lumps together the MAI and channel noise: $\mathbf{v}(m)=\sum_{k=2}^{K}\mathbf{A}_k(\boldsymbol{\tau}_k)\mathbf{b}_k(m)+\mathbf{e}(m)$. Due to the presence of $\mathbf{v}(m)$, the observed signal $\mathbf{y}(m)$ is "noisy," particularly when some user transmissions are significantly stronger than that of the desired user (i.e., in a near-far scenario). Hence, instead of directly using the raw data, we propose to first pass $\mathbf{y}(m)$ through a bank of filters (or filterbank), which are designed to enhance the useful signals and suppress the interference/noise and then derive the delay estimates from the filtered data. The proposed scheme is detailed next.

We first design a bank of L_1 finite-duration impulse response (FIR) filters,[2] denoted by $\mathbf{G}_1\in\mathbb{C}^{NQ\times 2L_1}$, for data prefiltering. While alternative design schemes may exist, we choose $\mathbf{G}_1$ based on the following idea: If $\mathbf{G}_1$ is effective in canceling the interference/noise, the average power of the filterbank output should be small; meanwhile, to avoid the trivial solution $\mathbf{G}_1=\mathbf{0}$ and to prevent signal cancellation, we should enforce certain constraints on $\mathbf{G}_1$ such that it will pass the desired signals with little distortion. Hence, the design criterion may be chosen as follows:

$$\begin{aligned}\mathbf{G}_1&=\arg\min_{\mathbf{G}\in\mathbb{C}^{NQ\times 2L_1}}\frac{1}{M}\sum_{m=0}^{M-1}\left\|\mathbf{G}^H\mathbf{y}(m)\right\|^2\\&=\arg\min_{\mathbf{G}\in\mathbb{C}^{NQ\times 2L_1}}\operatorname{tr}\left\{\mathbf{G}^H\hat{\mathbf{R}}_y\mathbf{G}\right\}\\&\qquad\text{subject to } \mathbf{G}_1^H\mathbf{A}_1(\boldsymbol{\tau}_1)=\mathbf{I}_{2L_1}\end{aligned} \quad (16)$$

where $\hat{\mathbf{R}}_y$ denotes the sample covariance matrix

$$\hat{\mathbf{R}}_y\triangleq\frac{1}{M}\sum_{m=0}^{M-1}\mathbf{y}(m)\mathbf{y}^H(m) \quad (17)$$

and the constraint $\mathbf{G}_1^H\mathbf{A}_1(\boldsymbol{\tau}_1)=\mathbf{I}_{2L_1}$ ensures that each filter (i.e., one column of $\mathbf{G}_1$) will pass only one signal component [corresponding to one column of $\mathbf{A}_1(\boldsymbol{\tau}_1)$] undistorted with unit-gain, while completely eliminating intersymbol interference (ISI) caused by the other columns of $\mathbf{A}_1(\boldsymbol{\tau}_1)$. Using the Lagrange multiplier, the solution to the above constrained quadratic minimization problem is given by (see also, e.g., [23, p. 283])

$$\mathbf{G}_1(\boldsymbol{\tau}_1)=\hat{\mathbf{R}}_y^{-1}\mathbf{A}_1(\boldsymbol{\tau}_1)\left[\mathbf{A}_1^H(\boldsymbol{\tau}_1)\hat{\mathbf{R}}_y^{-1}\mathbf{A}_1(\boldsymbol{\tau}_1)\right]^{-1} \quad (18)$$

where the dependence on $\boldsymbol{\tau}_1$ of $\mathbf{G}_1$ was made explicit. Substituting (18) into (16), the minimized average power of the filterbank output is given by

$$\operatorname{tr}\left\{\left[\mathbf{A}_1^H(\boldsymbol{\tau}_1)\hat{\mathbf{R}}_y^{-1}\mathbf{A}_1(\boldsymbol{\tau}_1)\right]^{-1}\right\}\triangleq U_1(\boldsymbol{\tau}_1). \quad (19)$$

[2]We consider FIR filters for implementation simplicity.

Note that the average power of the filterbank output depends on the unknown delay $\boldsymbol{\tau}_1$. An intuitive estimate $\hat{\boldsymbol{\tau}}_1$ of $\boldsymbol{\tau}_1$ would be the one that maximizes $U_1(\boldsymbol{\tau}_1)$ over all possible delays since, if $\hat{\boldsymbol{\tau}}_1$ coincides with the true delay $\boldsymbol{\tau}_1$, the filterbank $\mathbf{G}_1$ incurs no signal cancellation and maximizes the signal strength at the filterbank output. However, this is rather involved due to the nonlinear nature of $U_1(\boldsymbol{\tau}_1)$. By the Schwarz inequality, we note that (dropping the dependence on $\boldsymbol{\tau}_1$ for notational brevity)

$$\begin{aligned}\mathrm{tr}^2(\mathbf{I}_{2L_1}) =&\mathrm{tr}^2\left[(\mathbf{A}_1^H\hat{\mathbf{R}}_y^{-1}\mathbf{A}_1)^{-1/2}(\mathbf{A}_1^H\hat{\mathbf{R}}_y^{-1}\mathbf{A}_1)^{1/2}\right]\\ \le&\mathrm{tr}\left[(\mathbf{A}_1^H\hat{\mathbf{R}}_y^{-1}\mathbf{A}_1)^{-1}\right]\mathrm{tr}\left[\mathbf{A}_1^H\hat{\mathbf{R}}_y^{-1}\mathbf{A}_1\right]\end{aligned}$$

with equality holds if and only if $\mathbf{A}_1^H\hat{\mathbf{R}}_y^{-1}\mathbf{A}_1$ is proportional to an identity matrix. It follows that $U_1(\boldsymbol{\tau}_1)$ is lower bounded by

$$U_1(\boldsymbol{\tau}_1)\ge\frac{4L_1^2}{\mathrm{tr}\left[\mathbf{A}_1^H(\boldsymbol{\tau}_1)\hat{\mathbf{R}}_y^{-1}\mathbf{A}_1(\boldsymbol{\tau}_1)\right]}.$$

Instead of maximizing $U_1(\boldsymbol{\tau}_1)$, we can maximize its lower bound to seek computational simplicity. It turns out that doing so leads to an estimate that is still *statistically consistent* in signal-to-noise ratio (SNR). In particular, we show in Section IV-B that the resulting estimate converges to the true $\boldsymbol{\tau}_1$ in the absence of channel noise.

Hence, we choose $\hat{\boldsymbol{\tau}}_1$, which maximizes the lower bound on $U_1(\boldsymbol{\tau}_1)$ or, equivalently, which minimizes the following:

$$\begin{aligned}\hat{\boldsymbol{\tau}}_1 &=\arg\min_{\boldsymbol{\tau}_1}\mathrm{tr}\left\{\mathbf{A}_1^H(\boldsymbol{\tau}_1)\hat{\mathbf{R}}_y^{-1}\mathbf{A}_1(\boldsymbol{\tau}_1)\right\}\\ &=\arg\min_{0\le\tau_{1,1}<\cdots<\tau_{1,L_1}<T_s}\sum_{l=1}^{L_1}V_1(\tau_{1,l})\end{aligned}\tag{20}$$

where

$$V_1(\tau)\triangleq\mathbf{a}_1^H(\tau)\hat{\mathbf{R}}_y^{-1}\mathbf{a}_1(\tau)+\bar{\mathbf{a}}_1^H(\tau)\hat{\mathbf{R}}_y^{-1}\bar{\mathbf{a}}_1(\tau).\tag{21}$$

Since the L_1 terms of the cost function in the second line of (20) have identical form and the delay parameters are distinct [see (14)], it follows that the delay estimates $\{\hat{\tau}_{1,l}\}_{l=1}^{L_1}$, which minimizes the cost function, are *the* L_1 *smallest local minima* of $V_1(\tau)$ over the duration $\tau\in[0,T_s)$. As we show next, the L_1 smallest minima of $V_1(\tau)$ can be easily obtained in a *closed-form, noniterative* fashion, utilizing only a sequence of simple *first-order polynomial rooting*.

Decompose the dummy variable τ into a multiple of T_i: $\tau=(p+\mu)T_i$. Define $NQ\times NQ$ shifting matrices

$$\mathbf{P}(p)\triangleq\begin{bmatrix}\mathbf{0}&\mathbf{I}_p\\ \mathbf{0}&\mathbf{0}\end{bmatrix},\quad \bar{\mathbf{P}}(p)\triangleq\begin{bmatrix}\mathbf{0}&\mathbf{0}\\ \mathbf{I}_{NQ-p}&\mathbf{0}\end{bmatrix}.$$

One can easily see that the acyclic left and right shift of the spreading codes, given in (7) and (8), respectively, can be expressed as

$$\mathbf{c}_k^l(p)=\mathbf{P}(p)\mathbf{c}_k,\quad \mathbf{c}_k^r(p)=\bar{\mathbf{P}}(p)\mathbf{c}_k.\tag{22}$$

It follows from (5), (6), and (22) that

$$\mathbf{a}_k(\tau)=\mathbf{F}_k(p)\boldsymbol{\mu},\quad \bar{\mathbf{a}}_k(\tau)=\bar{\mathbf{F}}_k(p)\boldsymbol{\mu}\tag{23}$$

where

$$\mathbf{F}_k(p)\triangleq[\,\mathbf{P}(p)\mathbf{c}_k,\quad \mathbf{P}(p+1)\mathbf{c}_k\,]\tag{24}$$

$$\bar{\mathbf{F}}_k(p)\triangleq[\,\bar{\mathbf{P}}(p)\mathbf{c}_k,\quad \bar{\mathbf{P}}(p+1)\mathbf{c}_k\,]\tag{25}$$

$$\boldsymbol{\mu}\triangleq[\,1-\mu,\quad \mu\,]^T.\tag{26}$$

In light of (23), the cost function in (21) can be equivalently expressed as

$$\begin{aligned}V_1(p,\mu) =&\boldsymbol{\mu}^T\left[\mathbf{F}_1^H(p)\hat{\mathbf{R}}_y^{-1}\mathbf{F}_1(p)+\bar{\mathbf{F}}_1^H(p)\hat{\mathbf{R}}_y^{-1}\bar{\mathbf{F}}_1(p)\right]\boldsymbol{\mu}\\ \triangleq&\boldsymbol{\mu}^T\boldsymbol{\Omega}(p)\boldsymbol{\mu}\end{aligned}\tag{27}$$

where $\boldsymbol{\Omega}(p)\triangleq\mathbf{F}_1^H(p)\hat{\mathbf{R}}_y^{-1}\mathbf{F}_1(p)+\bar{\mathbf{F}}_1^H(p)\hat{\mathbf{R}}_y^{-1}\bar{\mathbf{F}}_1(p)$. Since $\boldsymbol{\Omega}(p)$ is Hermitian, we have $\boldsymbol{\mu}^T\Im[\boldsymbol{\Omega}(p)]\boldsymbol{\mu}=0$. It follows that

$$V_1(p,\mu)=\boldsymbol{\mu}^T\Re[\boldsymbol{\Omega}(p)]\boldsymbol{\mu}.\tag{28}$$

Next, we observe that $\Re[\boldsymbol{\Omega}(p)]$ is a 2×2 symmetric matrix, which can be expressed as

$$\Re[\boldsymbol{\Omega}(p)]\triangleq\begin{bmatrix}\omega_1(p)&\omega_3(p)\\ \omega_3(p)&\omega_2(p)\end{bmatrix}.\tag{29}$$

Substituting (26) and (29) into (28) yields (we sometimes drop the dependence on p for notational simplicity)

$$V_1(p,\mu)=(\omega_1+\omega_2-2\omega_3)\mu^2+2(\omega_3-\omega_1)\mu+\omega_1\tag{30}$$

which is a second-order polynomial of μ. For a specific value p' of p, $\tau'=(p'+\mu')T_i$ may be a local minimum of $V_1(p,\mu)$ over the open interval $(p'T_i,p'T_i+T_i)$ if $0<\mu'<1$, and μ' is a root of the derivative

$$\frac{\partial V_1(p',\mu)}{\partial\mu}=2(\omega_1+\omega_2-2\omega_3)\mu+2(\omega_3-\omega_1).$$

Rooting the above first-order polynomial yields

$$\mu'=\frac{\omega_1(p')-\omega_3(p')}{\omega_1(p')+\omega_2(p')-2\omega_3(p')},\ \text{if } 0\le\mu'<1.\tag{31}$$

Thus, we can form a set $\mathcal{S}$ of candidates (for the delay estimates) that contain all *stationary points*, i.e., $\tau'=(p'+\mu')T_i$ for every p' in $\{0,\ldots,NQ-1\}$ and the corresponding μ', as given in (31). Note that $V_1(\tau)$ may not be differentiable at the boundary points $\tau'=p'T_i$ for $p'=0,\ldots,NQ-1$. Hence, $\mathcal{S}$ should contain these points that may achieve local minima of $V_1(\tau)$ as well. The L_1*smallest minima* are then determined by evaluating $V_1(\tau)$ at every candidate in $\mathcal{S}$ followed by a ranking. To facilitate the evaluation of $V_1(\tau)$ over the set $\mathcal{S}$, we may use the following equivalent expression that is simpler than (30):

$$V_1(\tau')=\begin{cases}\omega_1(p'), & \text{if } \tau'=p'T_i\\ \frac{\omega_3(p')-\omega_1(p')}{\omega_1(p')+\omega_2(p')-2\omega_3(p')}+\omega_1(p'), & \text{if } \tau'=(p'+\mu')T_i.\end{cases}$$

To summarize, the proposed code synchronization scheme consists of the following steps.

1) Compute the sample covariance matrix $\hat{\mathbf{R}}_y$ by (17) and its inverse (assuming $M\ge NQ$ such that the $\hat{\mathbf{R}}_y$ is invertible).

2) Form the cost function $V_1(\tau)$ as in (21). Compute the delay estimates $\{\hat{\tau}_{1,l}\}_{l=1}^{L_1}$ as the L_1 smallest minima over the interval $0 \leq \tau < T_s$ by the approach described above.

Several remarks regarding the above implementation are necessary. First, we note that the only significant matrix manipulation of the proposed scheme is the forming of $\hat{\mathbf{R}}_y^{-1}$. A direct, batch-mode computation would require about $(NQ)^3$ operations. When implemented recursively using a standard RLS algorithm, the complexity can be reduced to $(NQ)^2$ (cf. Section IV-A). Even linear complexity RLS algorithms exist; see, for example, [24]. In forming the cost function (27), it should be noted that $\mathbf{P}(p)$ and $\bar{\mathbf{P}}(p)$ are shifting matrices. As a result, $\mathbf{F}_k(p)$ and $\bar{\mathbf{F}}_k(p)$ will be computed by shifting the spreading code $\mathbf{c}_k$ and not by direct matrix-vector multiplications. In addition, the 2×2 matrix $\boldsymbol{\Omega}(p)$ can be obtained by exploiting the fact that $\mathbf{F}_k(p)$ and $\bar{\mathbf{F}}_k(p)$ consist of only ± 1 and 0, and hence, no multiplications are necessary.

IV. Discussions

We remark that the only required knowledge by the proposed filterbank-based blind code synchronization scheme is the spreading code of the desired user. Therefore, it is good for a decentralized implementation. It does not need to know the number of active users, which is, however, indispensable to the subspace-based blind code synchronization scheme [9], [10] such that the signal subspace can be correctly separated from the noise subspace (also see Section V). Even the knowledge of the number of paths of the desired user is not critical to our scheme since an over- or under-determination of L_1 does not affect the delay estimates of the correctly detected paths. This is simply because the cost function $V_1(\tau)$ in (21) is independent of the parameter L_1. Of course, an over-determination of L_1 will result in delay estimates for spurious paths, while an under-determination of L_1 will pick out only the strongest paths, missing the wicker ones.

In the sequel, we discuss a few additional properties for the proposed scheme and derive an unconditional Cramér-Rao bound (UCRB) for the blind estimation problem. We also relate the proposed scheme to some previous work on blind code synchronization.

A. Adaptive Implementations

The proposed scheme can be readily recursively implemented by using the matrix inversion lemma, thus making it appealing for not only *code acquisition* but *code tracking* as well. Specifically, we can use the standard recursive least-squares (RLS) like iteration with forgetting factor $\kappa \in [0, 1]$ [24]:

$$\begin{aligned}\hat{\mathbf{R}}_y(m) =& \kappa \hat{\mathbf{R}}_y(m-1) + (1-\kappa)\mathbf{y}(m)\mathbf{y}^H(m)\\ \hat{\mathbf{R}}_y^{-1}(m) =& \frac{1}{\kappa}\hat{\mathbf{R}}_y^{-1}(m-1)\\ &- \frac{1-\kappa}{\kappa^2}\frac{\hat{\mathbf{R}}_y^{-1}(m-1)\mathbf{y}(m)\mathbf{y}^H(m)\hat{\mathbf{R}}_y^{-1}(m-1)}{1+(1-\kappa)\mathbf{y}^H(m)\hat{\mathbf{R}}_y^{-1}(m-1)\mathbf{y}(m)}\end{aligned}$$

where $\hat{\mathbf{R}}_y(m)$ denotes the sample covariance matrix based on the observed data up to and including $\mathbf{y}(m)$. Alternatively, we can also use a sliding window of length M symbol durations:

$$\begin{aligned}\hat{\mathbf{R}}_y(m) = & \hat{\mathbf{R}}_y(m-1)\\ &+ M^{-1}\left[\mathbf{y}(m)\mathbf{y}^H(m) - \mathbf{y}(m-M)\mathbf{y}^H(m-M)\right].\end{aligned}$$

In this case, $\hat{\mathbf{R}}_y^{-1}(m)$ can be recursively computed as (by applying the matrix inversion lemma twice)

$$\begin{aligned}\hat{\mathbf{R}}_y^{-1}(m) =& \hat{\mathbf{Q}}_y^{-1}(m)\\ &+ \frac{\hat{\mathbf{Q}}_y^{-1}(m)\mathbf{y}(m-M)\mathbf{y}^H(m-M)\hat{\mathbf{Q}}_y^{-1}(m)}{M-\mathbf{y}^H(m-M)\hat{\mathbf{Q}}_y^{-1}(m)\mathbf{y}(m-M)}\\ \hat{\mathbf{Q}}_y^{-1}(m) \triangleq& \hat{\mathbf{R}}_y^{-1}(m-1)\\ &- \frac{\hat{\mathbf{R}}_y^{-1}(m-1)\mathbf{y}(m)\mathbf{y}^H(m)\hat{\mathbf{R}}_y^{-1}(m-1)}{M+\mathbf{y}^H(m)\hat{\mathbf{R}}_y^{-1}(m-1)\mathbf{y}(m)}.\end{aligned}$$

Either one of the above adaptive implementations will lead to a complexity of the proposed scheme similar to that of the MMSE timing estimator with the RLS adaptation [5]. On the other hand, the subspace-based scheme [9], [10] requires an eigendecomposition of the $NQ \times NQ$ covariance matrix, which is computationally demanding. Although subspace tracking is also possible, it in, in general, more involved than the proposed scheme.

B. Statistical Consistency

The proposed filterbank scheme has another desired property: The delay estimates converge to the true delay parameters as the SNR increases, i.e., they are *statistically consistent*. This holds true, irrespective of the strength of the MAI (hence, the proposed scheme is *near–far resistant*) and for *finite* number of data samples. Specifically, we have the following result.

Proposition 1: Let

$$\mathbf{A}(\boldsymbol{\tau}) \triangleq [\mathbf{A}_1(\boldsymbol{\tau}_1), \quad \ldots, \quad \mathbf{A}_K(\boldsymbol{\tau}_K)] \in \mathbb{C}^{NQ\times 2L} \quad (32)$$

$$\mathbf{b}(m) \triangleq [\mathbf{b}_1^T(m), \quad \ldots, \quad \mathbf{b}_K^T(m)]^T \quad (33)$$

where $\boldsymbol{\tau} \triangleq [\boldsymbol{\tau}_1^T, \ \ldots, \boldsymbol{\tau}_K^T]^T$, and $L \triangleq \sum_{k=1}^{K} L_k$ denotes the total number of paths of all users. Assume the following.

A1) The noise samples are zero-mean and independently and identically distributed (i.i.d.) such that $E\{\mathbf{e}(m_1)\mathbf{e}^H(m_2)\} = \sigma_e^2 \mathbf{I}_{NQ}\delta(m_1 - m_2)$, where $\delta(m)$ denotes the Kronecker delta function, and σ_e^2 denotes the noise variance.

A2) $\mathbf{A}(\boldsymbol{\tau})$ has full column rank for all possible delays [i.e., $\mathbf{A}(\boldsymbol{\tau})$ is unambiguous].

A3) The matrix $\hat{\mathbf{R}}_b \triangleq 1/M\sum_{m=0}^{M-1}\mathbf{b}(m)\mathbf{b}^H(m)$ has full rank.

Then, the delay estimates given by (20) are statistically consistent (in SNR).

Proof: See Appendix A. ∎

We note that Assumption A1 is rather standard. Assumption A2 is needed to prevent ambiguity in the blind estimation problem under study. It requires that $NQ > 2L$ such that $\mathbf{A}(\boldsymbol{\tau})$ is a tall matrix; furthermore, the spreading codes and their shifts are required to be linearly independent of each other. Assumption A3 corresponds to the so-called "persistence-of-excitation" condition usually assumed in blind estimation problem (see [25]). It can be met as a results of, e.g., independent symbol emission and independent channel fading.

C. Intercell and Narrowband Interference Suppression

Since the proposed code synchronization scheme does not model the interference/noise term $\mathbf{v}(m)$ in (15) exactly, $\mathbf{v}(m)$ may contain *colored* noise and interference other than MAI, such as *intercell interference* and *narrowband interference* [12]. The overall interference/noise can be suppressed by the filterbank $\mathbf{G}_1$. On the other hand, the subspace-based code synchronization scheme [9], [10] assumes an *exact* parametric data model; it is sensitive to the presence of colored noise and *unmodeled* interference. The behavior of the two schemes under model mismatch is further investigated in Section V by computer simulations.

D. Unconditional Cramér–Rao Bound

The Cramér–Rao bound (CRB) conditioned on the transmitted data symbols and channel fading for the code timing estimation problem was derived and compared with the subspace-based timing estimator in [15]. Since blind algorithms assume no knowledge of the information symbols and channel fading, they are not expected to achieved the *conditional CRB*.[3] Here, we consider the CRB that is not conditioned on the information symbols nor the channel fading (hence, the name *unconditional CRB*, or *UCRB*). The UCRB is averaged over the unknown information symbols and channel fading and provides a lower bound for unbiased blind estimators.

To present the UCRB, the unknown parameters implicit in the estimation problem are first summarized. Let $\boldsymbol{\theta}_\tau \triangleq \left[\boldsymbol{\tau}_1^T, \ldots, \boldsymbol{\tau}_K^T\right]^T$ and $\boldsymbol{\theta}_P \triangleq [P_{1,1}, \ldots, P_{1,L_1}, \ldots, P_{K,1}, \ldots, P_{K,L_K}]^T$, where $P_{k,l} \triangleq E\{|\alpha_{k,l}(m)|^2\}$, $l = 1, \ldots, L_k$, which is the average received power associated with the lth path of user k. Let

$$\begin{aligned}\boldsymbol{\theta}_e \triangleq [r_e(0),\ \Re\{r_e(1)\},\ \Im\{r_e(1)\},\ \ldots \\ \Re\{r_e(NQ-1)\}, \Im\{r_e(NQ-1)\}]^T\end{aligned}$$

where $r_e(k)$ denotes the autocorrelation of the noise samples: $r_e(k) \triangleq E\{e(n)e^*(n-k)\}$. Since $\{e(n)\}$ is assumed stationary, $\mathbf{R}_e$ is Hermitian and Toeplitz and, thus, can be parameterized by its first column or, equivalently, $\boldsymbol{\theta}_e$, which is formed from the real and imaginary parts of the first column. We next form $\boldsymbol{\theta}$ consisting of all the unknown parameters:

$$\boldsymbol{\theta} \triangleq [\boldsymbol{\theta}_\tau^T, \quad \boldsymbol{\theta}_P^T, \quad \boldsymbol{\theta}_e^T]^T \in \mathbb{R}^{(2L+2NQ-1)\times 1}$$

where we recall $L \triangleq \sum_{k=1}^K L_k$. With the above definitions, the UCRB for $\boldsymbol{\theta}$ can be derived by using the Slepian–Bangs formula (e.g., [23]). In particular, we show in Appendix B that the UCRB matrix is given elementwise by

$$[UCRB^{-1}(\boldsymbol{\theta})]_{i,j} = M\mathrm{tr}\left[\mathbf{R}_y^{-1}\frac{\partial \mathbf{R}_y}{\partial[\boldsymbol{\theta}]_i}\mathbf{R}_y^{-1}\frac{\partial \mathbf{R}_y}{\partial[\boldsymbol{\theta}]_j}\right] \tag{34}$$

[3] It would be more appropriate to compare training-assisted schemes with the conditional CRB.

where $\mathbf{R}_y \triangleq E\{\mathbf{y}(m)\mathbf{y}^H(m)\}$, and the partial derivatives with respect to individual parameters are given by (38)–(40).

E. Relation to Previous Work

There are several previous studies related to the proposed filterbank approach. In particular, a minimum-variance criterion similar to (21) was considered in [19] for code synchronization in the downlink of CDMA systems. Unlike the strict derivation we presented in Section III, the discussion in [19] was made on a somewhat heuristic basis. For example, the timing uncertainty therein was *discretized* or *hypothesized* to form a *finite* set; furthermore, the path delay was assumed to be within that set. The cost function was then evaluated at each element of that set, and the one yielding the maximum of the cost function over the set was taken as the delay estimate. Apparently, the accuracy of this method is affected by how fine the time discretization is performed. Since the time-discretization induced error is independent of the SNR, the error will not vanish as the SNR increases. Hence, the so-obtained delay estimate is, in general, *statistically inconsistent*, which is in contrast to the *consistent* estimate produced by our scheme.

Perhaps [18] was the first to utilize the minimum-variance criterion for code synchronization in frequency-nonselective, time-invariant channels. To facilitate joint symbol demodulation, it was suggested therein to process data vectors formed from samples within two symbol intervals (as opposed to one symbol interval in our scheme). This leads to a higher computational complexity and a slower convergence rate of the synchronization algorithm. Time discretization was also employed therein for delay estimation. Additionally, as noted by the author, the algorithm involves a user parameter that is usually difficult to choose in practice.

The proposed filterbank-based scheme overcomes the difficulties of the above-mentioned methods. We will also stress that time-varying channel fading has been *explicitly* incorporated in our data model. As a result, the proposed scheme can cope with very fast channel fading, as also confirmed by the simulation results in Section V.

Finally, we remark that the filterbank approach is quite general. Indeed, different choices of the filterbank will, in general, lead to different synchronization schemes. The synchronization accuracy, however, will be mainly determined by how well the filterbank performs interference suppression. This suggests that other code synchronization schemes via alternative filterbank design with better interference cancellation ability may exist, and they have yet to be discovered.

V. Numerical Simulations

We consider a K-user asynchronous DS-CDMA system using a unit-energy binary phase shift keying (BPSK) constellation. Each user is assigned an $N = 31$ Gold code consisting of 1 and -1. To model both small- and large-scale fading, we decompose the fading coefficient into two parts and generate them separately: $\alpha_{k,l}(m) = \gamma_{k,l}(m)P_{k,l}$, where $\gamma_{k,l} \sim \mathcal{CN}(0,1)$ models the small-scale Rayleigh fading, whereas $P_{k,l}$ follows a log normal distribution to emulate the large-scale path loss and shadowing [26]. In the sequel, we consider near–far environments without enforcing stringent power control, where the total (from all paths) average power for the desired user is scaled so that $P_1 \triangleq \sum_{l=1}^{L_1} P_{1,l} = 1$, whereas the power for the $K-1$ interfering users follows a log normal distribution with a mean power $\bar{P}$ dB higher than that of the desired user. The near–far ratio (NFR) is defined as $\bar{P}$ (in decibels).

We consider both time-invariant and time-varying channels. In the former case, $\alpha_{k,l}$ and $P_{k,l}$ are generated according to the above-stated distributions, fixed for one experiment, but varied independently from trial to trial. In the time-varying case, $\alpha_{k,l}$ are functions of time, generated according to the Jakes' model [27] (also see discussions in Section V-B).

The average SNR for the desired user is defined as (recall that $P_1 = 1$)

$$\mathrm{SNR} \triangleq \frac{NQ}{\frac{1}{2\pi}\int_{-\pi}^{\pi}\phi(\omega)d\omega} \tag{35}$$

where $\phi(\omega)$ is the power spectral density (PSD) of the noise/interference sample [cf. (2)]: $e(n) \triangleq 1/T_i \int_{(n-1)T_i}^{nT_i} e(t)dt$. For bandlimited white Gaussian noise, (35) reduces to $\mathrm{SNR} = NQ/\sigma_e^2$, where σ_e^2 denotes the variance of $e(n)$. The primary performance measure is the *probability of correct acquisition*, which is defined as the probability of the event that the delay estimate is within a half chip of the true delay. Another performance measure is the root mean squared error (RMSE), which is normalized by T_c, of the delay estimate given correct acquisition. All results shown below are based on 400 Monte Carlo trials, where $\tau_{k,l}$ (delay), $\gamma_{k,l}$ (small-scale fading), $P_{k,l}$ (large-scale fading) for $k \neq 1$, $d_k(m)$ (symbols), and channel noise are varied independently from trial to trial.

A. Colored Noise and Intercell Interference

We first consider the case when $e(n)$ is *colored*, generated by a first-order autoregressive (AR) noise: $e(n) = 0.99e(n-1) + w(n)$, where $w(n)$ is a zero-mean white Gaussian process. The channel is assumed frequency-flat and time-invariant during acquisition. Fig. 1 shows the probability of correct acquisition of the proposed filterbank scheme and the subspace-based method [9], [10] as a function of the SNR when $K = 8$, $M = 150$, and $\mathrm{NFR} = 10$ dB. Both the chip-rate sampling ($Q = 1$) and oversampling ($Q = 2$) are considered. We see that in the presence of colored channel noise, the filterbank scheme outperforms the subspace method, especially when SNR is moderate or low (less than 20 dB).

The subspace method is known to be suboptimal in colored noise. It is natural to compare the two methods in channels with white noise. Fig. 2 depicts the performance in such a situation where all other simulation parameters remain unchanged, except that $e(n)$ is now a *white* noise. It is seen that the subspace method ($Q = 1$) outperforms the proposed method ($Q = 1$) for low SNR; however, when oversampling is utilized, the proposed scheme ($Q = 2$) yields almost identical performance to that of the subspace method ($Q = 2$).

In Fig. 2, we also simulate a scenario involving intercell interference (ICI) by letting two out of $K = 8$ transmissions be originated from some neighboring cells. We assume that the

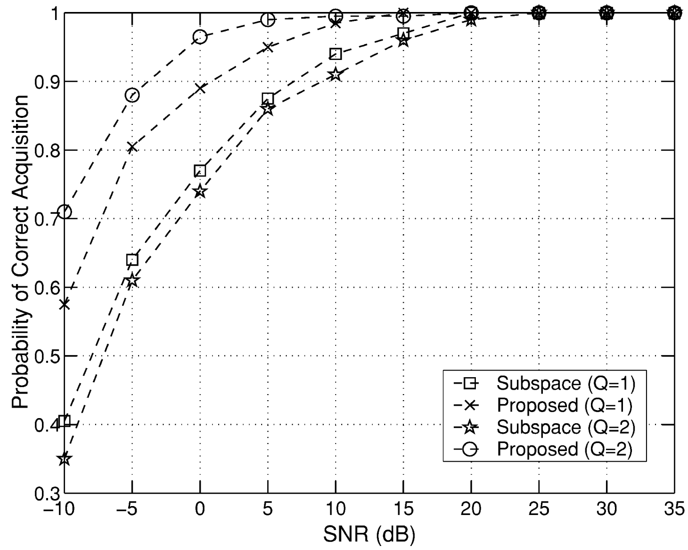

Fig. 1. Probability of acquisition versus SNR when $K = 8$, $M = 150$, and NFR$= 10$ dB in frequency-flat time-invariant channels with *colored* noise.

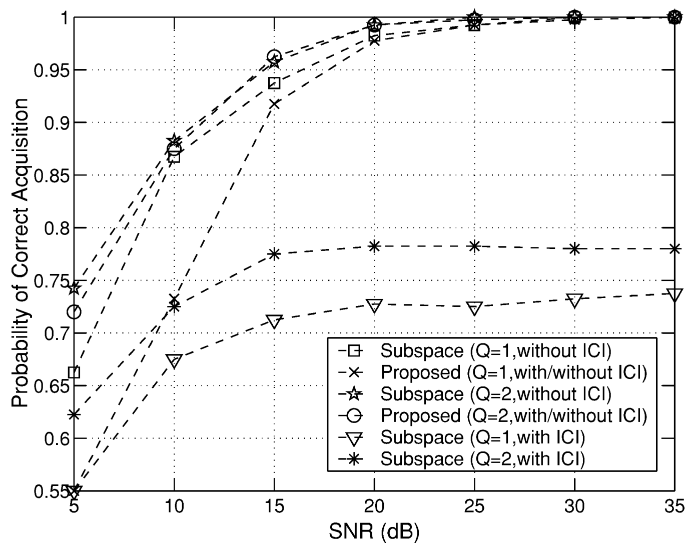

Fig. 2. Probability of acquisition versus SNR when $K = 8$, $M = 150$, and NFR$= 10$ dB in frequency-flat time-invariant channels with *white* noise.

subspace method, being unaware of the presence of ICI, uses $K = 6$ for synchronization (due to, e.g., a mis-estimation of the number of transmissions). We see that the subspace method degrades significantly in the presence of ICI. Meanwhile, the performance of the proposed scheme is independent of the transmission number (as long as the overall interference level remains the same) and, thus, is not affected by the ICI.

B. Fading Rate

Next, we examine the effect of channel variations on the proposed and subspace methods. To this end, frequency-flat time-varying Rayleigh fading channels are simulated. The channel fading $\alpha_{k,l}(t)$ [cf. (1)] is modeled as a zero-mean Gaussian stationary process with the classical U-shape PSD and unit power [27]. It is parameterized by the *normalized Doppler rate* $f_D T_s$, where f_D is the maximum Doppler rate and T_s the symbol interval. In our simulations, the fading process is generated by

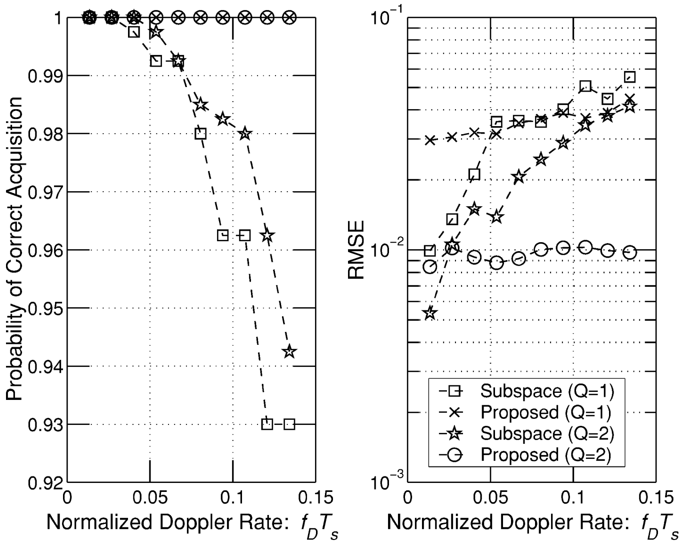

Fig. 3. (left) Probability of acquisition and (right) RMSE versus the normalized Doppler rate $f_D T_s$ when $K = 8$, $M = 150$, SNR $= 20$ dB, and NFR$= 10$ dB in frequency-flat channels.

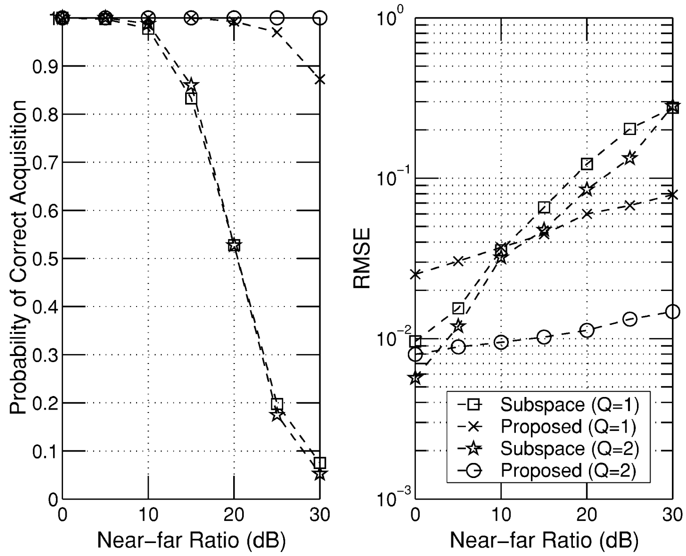

Fig. 4. (left) Probability of acquisition and (right) RMSE versus NFR when $K = 8$, $M = 150$, and SNR$= 20$ dB in frequency-flat time-varying channels with $f_D T_s = 0.08$.

the Jakes' model [27] and updated continuously every T_i s, where $T_i = T_c/Q$ is the sampling interval. As a result, the fading does not remain unchanged within a symbol interval, as assumed in Section II. Fig. 3 depicts (left) the probability of correct acquisition and (right) RMSE of the proposed and subspace methods as a function of $f_D T_s$, when $K = 8$, $M = 150$, SNR$= 20$ dB, NFR$= 10$ dB, and the channel noise is white. The result shows that the proposed scheme is extremely robust to time-varying fading, yielding no acquisition failure for all fading rates, whereas the subspace method degrades considerably as the fading rate increases. We also note that the subspace method produces slightly better RMSE when the channel is close to being stationary (i.e., small $f_D T_s$).

A comparison of Figs. 2 and 3 reveals that the proposed scheme actually achieves improved performance in time-varying channels than in time-invariant channels. The improvement comes from additional *time diversity* implicit in time-varying channels. To see this, we first remark that the performance of the proposed (as well as the subspace) scheme is primarily determined by the *effective* SNR for the desired user. Recall that $\gamma_{1,l}$, the (small-scale) fading coefficient associated with path l of user 1, is a Gaussian random variable that is fixed in one experiment but varied independently from trial to trial in the time-invariant case. The magnitude of $\gamma_{1,l}$, which determines the effective SNR for user 1, has a Rayleigh distribution and, therefore, is less than 0.5 with probability 0.2212.[4] That is, the effective SNR of the desired user is at least 6 dB smaller than the nominal average SNR for about 22.12% of the total (which is 400 in our simulations) trials in the time-invariant case. As one can expect, the probability of correct acquisition in these fading-impaired trials would be significantly lower than in the others, which degrades the overall performance. On the other hand, in the time-varying case with sufficiently fast fading rate, the channel is rarely locked at a deep fade throughout one trial. For example, at $f_D T_s = 0.08$, we have observed that the "down" time is typically less than 30% of the transmission time. Thus, channel variations provide the remarkable time diversity that may be exploited to improve performance. We note, however, that while the proposed scheme is able to benefit from channel fading, most training-assisted synchronization schemes suffer from it. As shown in [6], a relatively small Doppler rate (e.g., $f_D T_s = 0.008$) breaks down most well-known training-based schemes.

[4]The cumulative distribution function of $|\gamma_{1,l}|$ is $F(|\gamma_{1,l}|) = 1 - e^{-|\gamma_{1,l}|^2}$ [22, p. 45].

C. Near–Far Resistance

To test the performance of the proposed and subspace schemes in near-far environments, we consider a scenario where $K = 8$, $M = 150$, SNR$= 20$ dB, and the underlying channel is frequency-flat time-varying with $f_D T_s = 0.08$. Fig. 4 depicts (left) the probability of correct acquisition and (right) RMSE when the NFR is varied from 0 to 30 dB. It is seen that performance of the proposed scheme is relatively insensitive to the NFR, whereas the subspace method degrades significantly as the NFR increases. We note that with power control and thus small NFR, the subspace method may yield slightly better RMSE.

D. User Capacity

We next examine the user capacity of the proposed and subspace schemes in time-varying, frequency-flat, and frequency-selective channels. For frequency-selective channels, we assume that each user transmission undergoes two independent paths with equal (average) power before reaching the receiver. We declare correct acquisition in the multipath case whenever the delay estimate of the path of interest is within a half chip to the true delay, regardless of the delay estimate of the other path. Nevertheless, we have noticed similar performance for both paths, in terms of both the probability of acquisition and RMSE, primarily because each path carries similar average

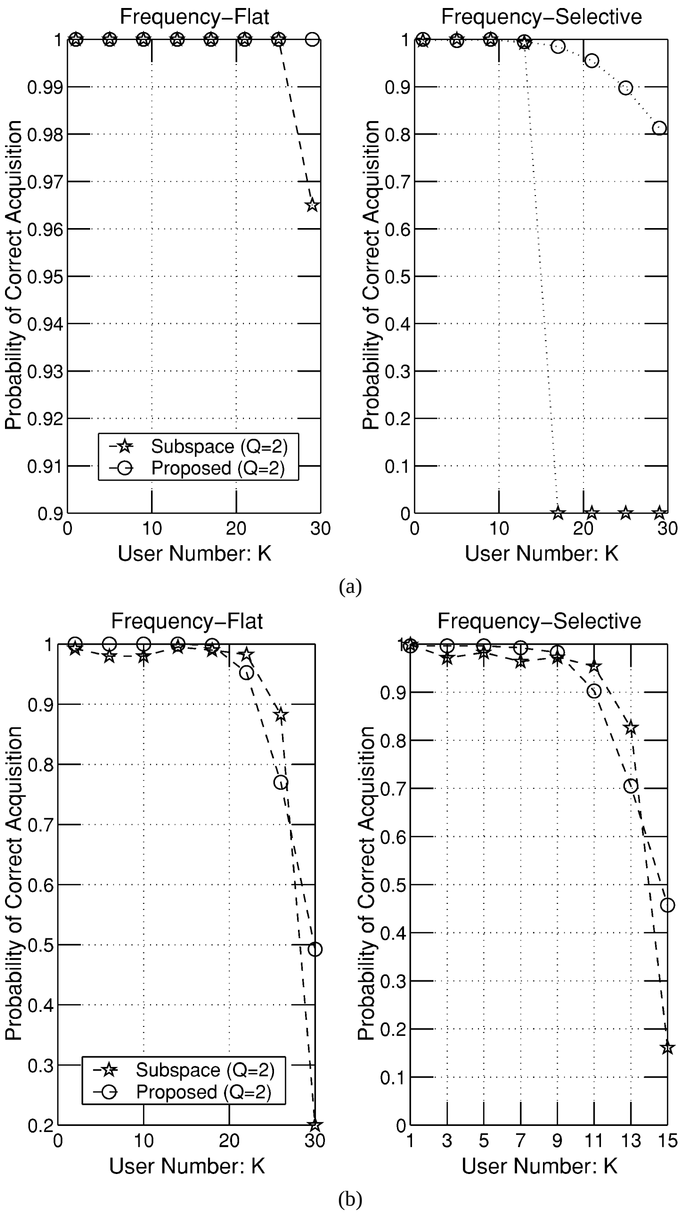

Fig. 5. Probability of acquisition versus K, the number of users when $M = 150$ and SNR $= 20$ dB in (left) frequency-flat and (right) frequency-selective, time-varying channels with $f_D T_s = 0.08$. (a) NFR= 0 dB. (b) NFR= 10 dB.

power. Accordingly, instead of showing the results for each path separately, we only show the average of the probability of acquisition (or RMSE) of the two paths. During our simulations, we have also observed that the proposed as well as the subspace methods occasionally produce two path delay estimates that are very close to one another, with a difference typically less than $0.1T_c$. Since such a relative delay is not resolvable in practice unless additional bandwidth is available, whenever this occurs, we discard one of the two estimates and use the next candidate in $\mathcal{S}$, which we recall is formed by all candidates, or the local minima of the cost function for the proposed scheme [see the discussions following (31)].

We first consider the scenario when $M = 150$, SNR= 20 dB, and NFR= 0 dB. Fig. 5(a) depicts the results for (left) frequency-flat and (right) frequency-selective channels. We see that in both cases, the proposed scheme surpasses the subspace

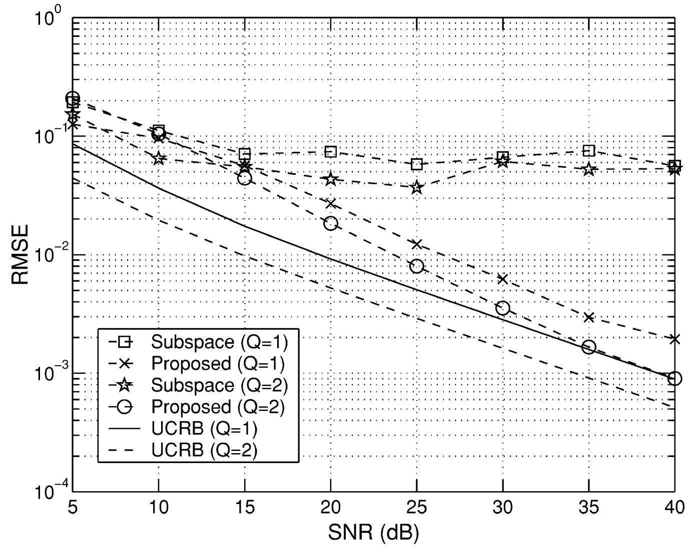

Fig. 6. RMSE and UCRB versus SNR when $K = 4$, $M = 150$, and NFR= 10 dB in frequency-selective time-varying channels with $f_D T_s = 0.08$.

method with a larger capacity. The subspace method has a limited capacity in multipath channels due to the so-called interference dimension problem. In particular, assuming that each of the K users undergoes L_0 paths, the maximum number of users that can be supported by the subspace method must satisfy $K < NQ/(2L_0)$ in order to ensure nontrivial noise subspace (see also [7]). For $N = 31$ and $Q = 2$, this implies that the subspace can support up to $K = 30$ users in single-path channels and $K = 15$ users in two-path channels, respectively, as also confirmed in Fig. 5(a). On the other hand, the proposed scheme is not limited by the above interference dimension problem and has a larger user capacity than the subspace method.

We note, however, that the user capacity of the proposed scheme is affected by the overall interference level. Fig. 5(b) depicts the results of the two methods in a more difficult scenario with simulation parameters similar to those in Fig. 5(a), except that NFR= 10 dB (for all interfering users). In the current case, the proposed method is seen to have a similar user capacity to that of the subspace method. We also see that for small-to-medium values of K, the performance of the subspace scheme fluctuates quit a bit, whereas the proposed scheme maintains an ideal performance with a probability of acquisition equal to one.

E. UCRB

The last example compares the RMSE of the timing estimates with the UCRB in (34). Fig. 6 depicts the RMSE and UCRB when $K = 4$, $M = 150$, and NFR= 10 dB in frequency-selective (two-path), time-varying channels with $f_D T_s = 0.08$. Since the UCRB is a function of the delay parameters, these parameters are fixed through the 400 Monte Carlo trials, whereas the other parameters are varied independently from trail to trial, like the previous examples. It is seen that the proposed scheme approaches the UCRB as the SNR increases. On the other hand, the subspace method is far away from the UCRB, with an irreducible estimation error suggesting that it may be statistically inconsistent.

VI. Conclusions

We proposed a filterbank-based blind code synchronization scheme for asynchronous DS-CDMA systems. The proposed scheme requires only the spreading code of the desired user. It can be efficiently recursively implemented for both code acquisition and code tracking. The proposed scheme yields statistically consistent delay estimates under mild conditions. It is versatile since it is applicable to diverse fading environments such as single-path and multipath, time-invariant, and time-varying channels. Furthermore, it can deal with colored channel noise and interference of various origins, including MAI, ISI, ICI, and narrowband interference. We also derived a UCRB, which serves as a lower bound for all unbiased blind code synchronization algorithms.

The filterbank scheme is rather general in the sense that different choices of the filterbank lead to different code synchronizer. Although other code synchronization schemes based on alternative filterbank designs have yet to be discovered, it certainly remains an interesting topic that merits future investigation.

We focused on rectangular chip waveforms throughout this paper. To consider bandlimited chip waveforms (e.g, square-root raised-cosine pulses), we can first apply Fourier transform on the received signal and then perform a deconvolution in the frequency domain (see, e.g., [28] and [29]). After the chip-pulse deconvolution, it is conceivable that a similar filterbank approach can be devised for code timing estimation (which reduces to frequency estimation in this case) in the frequency domain. We are exploring such a direction and will report our finding in the near future.

Appendix A
Proof of Proposition 1

We first rewrite (11) as

$$\mathbf{y}(m) = \mathbf{A}(\boldsymbol{\tau})\mathbf{b}(m) + \mathbf{e}(m).$$

As the SNR increases, one can see that the limiting form of the sample covariance matrix is given by

$$\lim_{\sigma_e^2 \to 0} \hat{\mathbf{R}}_y = \mathbf{A}(\boldsymbol{\tau})\hat{\mathbf{R}}_b\mathbf{A}^H(\boldsymbol{\tau}).$$

The above expression, along with Assumptions A1–A3, suggests that the eigendecomposition of the limiting sample covariance matrix can be expressed as

$$\lim_{\sigma_e^2 \to 0} \hat{\mathbf{R}}_y = [\,\mathbf{E}_s, \quad \mathbf{E}_n\,] \begin{bmatrix} \boldsymbol{\Lambda}_s & \mathbf{0} \\ \mathbf{0} & \mathbf{0} \end{bmatrix} \begin{bmatrix} \mathbf{E}_s^H \\ \mathbf{E}_n^H \end{bmatrix}$$

where $\boldsymbol{\Lambda}_s \in \mathbb{R}^{2L\times 2L}$ is a diagonal matrix made from the $2L$ nontrivial eigenvalues, $\mathbf{E}_s \in \mathbb{C}^{NQ\times 2L}$ contains the associated eigenvectors, and $\mathbf{E}_n \in \mathbb{C}^{NQ\times(NQ-2L)}$ contains the eigenvectors corresponding to the zero-eigenvalue with multiplicity $NQ-2L$. We note that $\text{span}\{\mathbf{E}_s\} = \text{span}\{\mathbf{A}(\boldsymbol{\tau})\}$, whereas the left null space of $\mathbf{A}(\boldsymbol{\tau})$ is spanned by $\mathbf{E}_n$ (e.g., [30]).

At finite SNR, $\hat{\mathbf{R}}_y^{-1}$ can be expressed by the eigendecomposition of $\hat{\mathbf{R}}_y$:

$$\hat{\mathbf{R}}_y^{-1} = \hat{\mathbf{E}}_s\hat{\boldsymbol{\Lambda}}_s^{-1}\hat{\mathbf{E}}_s^H + \hat{\mathbf{E}}_n\hat{\boldsymbol{\Lambda}}_n^{-1}\hat{\mathbf{E}}_n^H$$

where $\hat{\boldsymbol{\Lambda}}_s$, $\hat{\mathbf{E}}_s$, $\hat{\boldsymbol{\Lambda}}_n$, and $\hat{\mathbf{E}}_n$ are known to converge uniformly to $\boldsymbol{\Lambda}_s$, $\mathbf{E}_s$, $\sigma_e^2\mathbf{I}_{NQ}$, and $\mathbf{E}_n$, respectively, as $\sigma_e^2 \to 0$[31]. Hence

$$\lim_{\sigma_e^2 \to 0} \sigma_e^2\hat{\mathbf{R}}_y^{-1} = \mathbf{E}_n\mathbf{E}_n^H.$$

It follows that the cost function in (20) can be written as

$$\begin{aligned} &\lim_{\sigma_e^2 \to 0} \sigma_e^2 \text{tr}\{\mathbf{A}^H(\boldsymbol{\tau}_1)\hat{\mathbf{R}}_y^{-1}\mathbf{A}^H(\boldsymbol{\tau}_1)\} \\ &= \text{tr}\{\mathbf{A}^H(\boldsymbol{\tau}_1)\mathbf{E}_n\mathbf{E}_n^H\mathbf{A}^H(\boldsymbol{\tau}_1)\} \\ &\triangleq \mathring{V}_1(\boldsymbol{\tau}_1). \end{aligned}$$

We note that the minimum $\mathring{V}1(\boldsymbol{\tau}_1) = 0$ is achieved if $\hat{\boldsymbol{\tau}}_1 = \boldsymbol{\tau}_1$. The uniqueness of this estimate follows from Assumption A2.

■

Appendix B
Unconditional Cramér–Rao Bound

Using the definitions (32) and (33), we rewrite (11) as follows:

$$\mathbf{y}(m) = \mathbf{A}(\boldsymbol{\tau})\mathbf{b}(m) + \mathbf{e}(m), \quad m = 0, \ldots, M-1.$$

We note that [cf. (9) and (10)]

$$\begin{aligned} \mathbf{R}_{b_k} &\triangleq E\{\mathbf{b}_k(m)\mathbf{b}_k^H(m)\} \\ &= \text{diag}\{\, P_{k,1}, \quad P_{k,1}, \quad \ldots, P_{k,L_k}, \quad P_{k,L_k}\,\} \end{aligned}$$

where $P_{k,l} \triangleq E\{|\alpha_{k,l}(m)|^2\}$, $l = 1, \ldots, L_k$, which is the average received power associated with the lth path of user k, and the fading processes $\{\alpha_{k,l}(m)\}_{l=1}^{L_k}$ are assumed stationary, zero-mean, independent of one another (with respect to different k or l), as well as independent of the information symbols $\{d_k(m)\}$; the information symbols are assumed to be i.i.d. and drawn from some unit-energy constellation, i.e., $E\{d_{k_1}(m_1)d_{k_2}^*(m_2)\} = \delta(k_1-k_2)\delta(m_1-m_2)$. With these assumptions, we can see that

$$\mathbf{R}_b \triangleq E\{\mathbf{b}(m)\mathbf{b}^H(m)\} = \text{diag}\{\,\mathbf{R}_{b_1}, \quad \ldots, \quad \mathbf{R}_{b_K}\,\}.$$

Although the assumptions made in the above are rather standard, we need a few additional ones in order to arrive at a simple but useful expression for the UCRB. In particular, we assume that the vectors $\{\mathbf{b}(m)\}_{m=0}^{M-1}$ are Gaussian with zero-mean and covariance matrix $E\{\mathbf{b}(m_1)\mathbf{b}(m_2)\} = \mathbf{R}_b\delta(m_1-m_2)$; furthermore, the noise vectors $\{\mathbf{e}(m)\}_{m=0}^{M-1}$ are assumed to to be independent of $\{\mathbf{b}(m)\}_{m=0}^{M-1}$ and follow a Gaussian distribution with zero-mean and covariance matrix $E\{\mathbf{e}(m_1)\mathbf{e}(m_2)\} = \mathbf{R}_e\delta(m_1-m_2)$. We will point out that $\mathbf{y}(m_1)$ and $\mathbf{y}(m_2)$ for different m_1 and m_2 may be correlated with each other, due to asynchronous transmissions. However, we ignore the correlation to make our derivation tractable. The exact distribution of $\{\mathbf{y}(m)\}$ is, in general, too complex to obtain. On the other hand, the CRB based on a Gaussian assumption is the lower bound for the covariance matrices of a large class of estimation methods, regardless of the data distribution [23, p. 293]. As such, it makes sense to compare with the CRB based on a Gaussian assumption.

Let $\mathbf{y} \triangleq [\mathbf{y}^T(0), \ldots, \mathbf{y}^T(M-1)]^T$. With the aforementioned assumptions, we have $\mathbf{y} \sim \mathcal{CN}(\mathbf{0}, \boldsymbol{\mathcal{R}}_y)$, where

$$\boldsymbol{\mathcal{R}}_y = \mathbf{I}_M \otimes \left[\mathbf{A}(\boldsymbol{\tau})\mathbf{R}_b\mathbf{A}(\boldsymbol{\tau})^H + \mathbf{R}_e\right] \triangleq \mathbf{I}_M \otimes \mathbf{R}_y. \quad (36)$$

According to the Slepian–Bangs formula, the UCRB matrix is given elementwise by (e.g., [23])

$$[\mathrm{UCRB}^{-1}(\boldsymbol{\theta})]_{i,j} = \mathrm{tr}\left[\boldsymbol{\mathcal{R}}_y^{-1}\frac{\partial \boldsymbol{\mathcal{R}}_y}{\partial[\boldsymbol{\theta}]_i}\boldsymbol{\mathcal{R}}_y^{-1}\frac{\partial \boldsymbol{\mathcal{R}}_y}{\partial[\boldsymbol{\theta}]_j}\right]. \quad (37)$$

Using (36), it is trivial to show that (37) can be simplified as (34).

We next calculate the partial differentiation w.r.t. each unknown parameter. First, consider the partial differentiation w.r.t. the delay parameters contained in $\boldsymbol{\theta}_\tau$:

$$\begin{aligned}\frac{\partial \mathbf{R}_y}{\partial \tau_{k,l}} &= \frac{\partial}{\partial \tau_{k,l}} P_{k,l}\left[\mathbf{a}_k(\tau_{k,l})\mathbf{a}_k^H(\tau_{k,l}) + \bar{\mathbf{a}}_k(\tau_{k,l})\bar{\mathbf{a}}_k^H(\tau_{k,l})\right]\\ &= \frac{\partial}{\partial \tau_{k,l}} P_{k,l}\left[\mathbf{F}_k(p_{k,l})\boldsymbol{\mu}_{k,l}\boldsymbol{\mu}_{k,l}^H\mathbf{F}_k^H(p_{k,l})\right.\\ &\quad \left.+ \bar{\mathbf{F}}_k(p_{k,l})\boldsymbol{\mu}_{k,l}\boldsymbol{\mu}_{k,l}^H\bar{\mathbf{F}}_k^H(p_{k,l})\right]\\ &= P_{k,l}\left[\mathbf{F}_k(p_{k,l})\mathbf{D}_{k,l}\mathbf{F}_k^H(p_{k,l}) + \bar{\mathbf{F}}_k(p_{k,l})\mathbf{D}_{k,l}\bar{\mathbf{F}}_k^H(p_{k,l})\right]\\ &\qquad k = 1, \ldots, K;\ l = 1, \ldots, L_k \end{aligned} \quad (38)$$

where the second equality follows from (23), $\mathbf{F}_k(p_{k,l})$, $\bar{\mathbf{F}}_k(p_{l,k})$, and $\boldsymbol{\mu}_{k,l}$ are similarly defined as in (24)–(26), respectively, and

$$\mathbf{D}_{k,l} \triangleq \frac{\partial(\boldsymbol{\mu}_{k,l}\boldsymbol{\mu}_{k,l}^H)}{\partial \tau_{k,l}} = \begin{bmatrix} 2(\mu_{k,l}-1) & 1-2\mu_{k,l} \\ 1-2\mu_{k,l} & 2\mu_{k,l} \end{bmatrix}.$$

Next, consider the partial differentiation w.r.t. the power parameters contained in $\boldsymbol{\theta}_P$:

$$\begin{aligned}\frac{\partial \mathbf{R}_y}{\partial P_{k,l}} &= \frac{\partial}{\partial P_{k,l}} P_{k,l}\left[\mathbf{a}_k(\tau_{k,l})\mathbf{a}_k^H(\tau_{k,l}) + \bar{\mathbf{a}}_k(\tau_{k,l})\bar{\mathbf{a}}_k^H(\tau_{k,l})\right]\\ &= \mathbf{a}_k(\tau_{k,l})\mathbf{a}_k^H(\tau_{k,l}) + \bar{\mathbf{a}}_k(\tau_{k,l})\bar{\mathbf{a}}_k^H(\tau_{k,l})\\ &\quad k = 1, \ldots, K;\ l = 1, \ldots, L_k. \end{aligned} \quad (39)$$

Finally, the partial differentiation w.r.t. the noise autocorrelation parameters contained in $\boldsymbol{\theta}_e$ is given by

$$\begin{aligned}\frac{\partial \mathbf{R}_y}{\partial[\boldsymbol{\theta}_e]_i} &= \frac{\partial \mathbf{R}_e}{\partial[\boldsymbol{\theta}_e]_i}\\ &= \begin{cases} \mathbf{I}_{NQ}, & i = 1\\ \mathbf{Q}_l + \mathbf{Q}_l^T, & i = 2l,\ l = 1, \ldots, NQ-1\\ j(\mathbf{Q}_l - \mathbf{Q}_l^T), & i = 2l+1,\ l = 1, \ldots, NQ-1 \end{cases} \end{aligned} \quad (40)$$

where

$$\mathbf{Q}_l \triangleq \begin{bmatrix} \mathbf{0} & \mathbf{0} \\ \mathbf{I}_{NQ-l} & \mathbf{0} \end{bmatrix}.$$

Substituting (38) –(40) in (34), the UCRB can be readily calculated.

REFERENCES

[1] R. Prasad and T. Ojanperä, "An overview of CDMA evolution toward wideband CDMA," *IEEE Commun Surveys*, vol. 1, no. 1, pp. 2–29, 1998.

[2] S. Verdú, *Multiuser Detection*. Cambridge, U.K.: Cambridge Univ. Press, 1998.

[3] R. F. Smith and S. L. Miller, "Code timing estimation in a near-far environment for direct-sequence code-division multiple-access," *Proc. IEEE Military Commun. Conf.*, pp. 47–51, 1994.

[4] U. Madhow, "Adaptive interference suppression for joint acquisition and demodulation of direct-sequence CDMA signals," *Proc. IEEE Military Commun. Conf.*, pp. 1200–1204, 1995.

[5] R. F. Smith and S. L. Miller, "Acquisition performance of an adaptive receiver for DS-CDMA," *IEEE Trans. Commun.*, vol. 47, pp. 1416–1424, Sept. 1999.

[6] H. Li, J. Li, and S. L. Miller, "Decoupled multiuser code-timing estimation for code-division multiple-access communication systems," *IEEE Trans. Commun.*, vol. 49, pp. 1425–1436, Aug. 2001.

[7] D. Zheng, J. Li, S. L. Miller, and E. G. Ström, "An efficient code-timing estimator for DS-CDMA system," *IEEE Trans. Signal Processing*, vol. 45, pp. 82–89, Jan. 1997.

[8] S. E. Bensley and B. Aazhang, "Maximum-likelihood synchronization of a single user for code-division multiple-access communication systems," *IEEE Trans. Commun.*, vol. 46, pp. 392–399, Mar. 1998.

[9] E. G. Ström, S. Parkvall, S. L. Miller, and B. E. Ottersten, "Propagation delay estimation in asynchronous direct-sequence code-division multiple access systems," *IEEE Trans. Commun.*, vol. 44, pp. 84–93, Jan. 1996.

[10] S. E. Bensley and B. Aazhang, "Subspace-based channel estimation for code division multiple access communications systems," *IEEE Trans. Commun.*, vol. 44, pp. 1009–1020, Aug. 1996.

[11] R. O. Schmidt, "Multiple emitter location and signal parameter estimation," *IEEE Trans. Antennas Propagat.*, vol. AP-34, pp. 276–280, Mar. 1986.

[12] H. V. Poor, "Active interference suppression in CDMA overlay systems," *IEEE J. Select. Areas Commun.*, vol. 19, pp. 4–20, Jan. 2001.

[13] M. Wax and T. Kailath, "Detection of signals by information theoretic criteria," *IEEE Trans. Acoust., Speech Signal Processing*, vol. ASSP-33, pp. 387–392, Apr. 1985.

[14] T. Söderström and P. Stoica, *System Identification*. London, U.K.: Prentice-Hall Int., 1989.

[15] E. G. Ström, S. Parkvall, S. L. Miller, and B. E. Ottersten, "DS-CDMA synchronization in time-varying fading channels," *IEEE J. Select. Areas Commun.*, vol. 14, pp. 1636–1642, Oct. 1996.

[16] T.Östman, S. Parkvall, and B. Ottersten, "An improved MUSIC algorithm for estimation of time delays in asynchronous DS-CDMA systems," *IEEE Trans. Commun.*, vol. 47, pp. 1628–1631, Nov. 1999.

[17] B. Farhang-Boroujeny, *Adaptive Filters: Theory and Applications*. Chichester, U.K.: Wiley, 1998.

[18] U. Madhow, "Blind adaptive interference suppression for the near-far resistant acquisition and demodulation of direct-sequence CDMA signals," *IEEE Trans. Signal Processing*, vol. 45, pp. 124–136, Jan. 1997.

[19] M. Latva-aho, J. Lilleberg, J. Iinatti, and M. Juntti, "CDMA downlink code acquisition performance in frequency-selective fading channels," *Proc. IEEE Int. Symp. Personal, Indoor Mobile Radio Commun.*, pp. 1476–1479, Sept. 1998.

[20] G. H. Golub and C. F. Van Loan, *Matrix Computations*, 3 ed. Baltimore, MD: Johns Hopkins Univ. Press, 1996.

[21] A. Graham, *Kronecker Products and Matrix Calculus with Applications*. Chichester, U.K.: Ellis Horwood, 1981.

[22] J. G. Proakis, *Digital Communications*, 3 ed. New York: McGraw-Hill, 1995.

[23] P. Stoica and R. L. Moses, *Introduction to Spectral Analysis*. Upper Saddle River, NJ: Prentice-Hall, 1997.

[24] S. Haykin, *Adaptive Filter Theory*, 3 ed. Upper Saddle River, NJ: Prentice-Hall, 1996.

[25] L. Tong and S. Perreau, "Multichannel blind identification: From subspace to maximum likelihood methods," *Proc. IEEE*, vol. 86, pp. 1951–1968, Oct. 1998.

[26] T. S. Rappaport, *Wireless Communications: Principles and Practice*. Upper Saddle River, NJ: Prentice-Hall, 1996.

[27] W. C. Jakes Jr, *Microwave Mobile Communications*. New York: Wiley-Interscience, 1974.

[28] A. Lee Swindlehurst, "Time delay and spatial signature estimation using known asynchronous signals," *IEEE Trans. Signal Processing*, vol. 46, pp. 449–462, Feb. 1998.

[29] A. J. van der Veen, M. C. Vanderveen, and A. Paulraj, "Joint angle and delay estimation using shift-invariance techniques," *IEEE Trans. Signal Processing*, vol. 46, pp. 405–418, Feb. 1998.
[30] M. Viberg, "Sensitivity of parametric direction finding to colored noise fields and undermodeling," *Signal Process.*, vol. 34, no. 2, pp. 207–222, Nov. 1993.
[31] G. W. Stewart and J.-G. Sun, *Matrix Perturbation Theory*, 3 ed. San Diego, CA: Academic, 1990.

Hongbin Li (M'99) received the B.S. and M.S. degrees from the University of Electronic Science and Technology of China (UESTC), Chengdu, in 1991 and 1994, respectively, and the Ph.D. degree from the University of Florida, Gainesville, in 1999, all in electrical engineering.

From July 1996 to May 1999, he was a Research Assistant with the Department of Electrical and Computer Engineering, University of Florida. Since July 1999, he has been an Assistant Professor with the Department of Electrical and Computer Engineering, Stevens Institute of Technology, Hoboken, NJ. His current research interests include stochastic signal processing, sensor array processing, wireless communications, and radar imaging.

Dr. Li is a member of Tau Beta Pi and Phi Kappa Phi. He received the Jess H. Davis Memorial Award for excellence in research from Stevens Institute of Technology in 2001 and the Sigma Xi Graduate Research Award from the University of Florida in 1999.

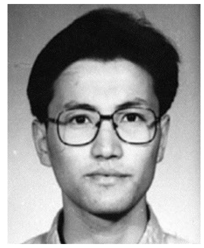

Rensheng Wang received the B.E. and M.E. degrees from Harbin Institute of Technology, Harbin, China, in 1995 and 1997, respectively, both in electrical engineering. He is currently pursuing the Ph.D. degree in electrical engineering with the Department of Electrical and Computer Engineering, Stevens Institute of Technology, Hoboken, NJ.

He is currently working as a research assistant with the Department of Electrical and Computer Engineering, at Stevens. From 1997 to 2000, he was a researcher at the Institute of Electronics, Chinese Academy of Sciences, Beijing, China. His research interests are in the area of signal processing for communications with focus on multiuser detection and estimation in code division multiple access.